

MLAAN: Scaling Supervised Local Learning with Multilaminar Leap Augmented Auxiliary Network

Yuming Zhang*, Shouxin Zhang*, Peizhe Wang*, Feiyu Zhu, Dongzhi Guan†, Jiabin Liu, Changpeng Cai†

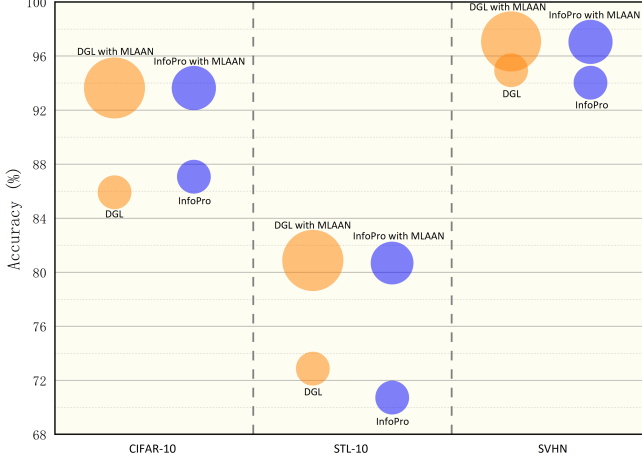


Fig. 1. Comparison between different methods with MLAAN and the original methods in terms of GPU Memory Usage and Accuracy. Results are obtained using ResNet-32 on the CIFAR-10, STL-10 and SVHN datasets. The diameter of each bubble is proportional to the GPU memory usage.

Abstract—End-to-end (E2E) training approaches are commonly plagued by high memory consumption, reduced efficiency in training, challenges in model parallelization, and suboptimal biocompatibility. Local learning is considered a novel interactive training method that holds promise as an alternative to E2E. Nonetheless, conventional local learning methods fall short in achieving high model accuracy due to inadequate local inter-module interactions. In this paper, we introduce a new model known as the Scaling Supervised Local Learning with Multilaminar Leap Augmented Auxiliary Network (MLAAN). MLAAN features an innovative supervised local learning approach coupled with a robust reinforcement module. This dual-component design enables the MLAAN to integrate smoothly with established local learning techniques, thereby enhancing the efficacy of the foundational methods. The method simultaneously acquires the local and global features of the model separately by constructing an independent auxiliary network and a cascade auxiliary network on the one hand and incorporates a leap augmented module, which serves to counteract the reduced learning capacity often associated with weaker supervision. This architecture not only augments the exchange of information amongst the local modules but also effectively mitigates the model’s tendency toward myopia. The experimental evaluations conducted on four benchmark datasets, CIFAR-10, STL-10, SVHN, and ImageNet, demonstrate that the integration of MLAAN with existing supervised local learning methods significantly enhances the original methodologies. Of particular note, MLAAN enables local learning methods to comprehensively outperform end-to-end training approaches in terms of optimal performance while saving GPU memory.

Index Terms—Auxiliary networks, leap augmented modules, multilaminar local modules, supervised local learning.

I. INTRODUCTION

As a mainstream method for training deep neural networks, end-to-end (E2E) backpropagation has achieved remarkable success in image segmentation [1], point cloud geometry compression [2], target tracking [3], referring expression segmentation [4], visual sound separation [5], and other fields. Despite these accomplishments, the E2E learning paradigm is not without its drawbacks. On one hand, the E2E training regimen necessitates the retention of the complete computational graph and all intermediate activations post each local module’s computation [6]. This requirement for substantial memory resources leads to escalated GPU memory usage during the training phase. As network depth and model intricacy expand, this surge in memory demand can severely constrain the training of sophisticated models that operate on high-resolution data inputs [7]. On the other hand, the inherent structure of E2E training mandates that initial layers await the propagation of loss values from subsequent layers. Consequently, parameters within the hidden layers are barred from updating until the entire forward and backward propagation cycles conclude, culminating in a less efficient model [8], [9]. Furthermore, the sequential nature of gradient processing in this context not only impedes model parallelization [10], [11] but also raises concerns regarding biological plausibility due to the dependency on cross-layer backpropagation for parameter weight updates [12], [13]. These issues collectively contribute to the limitations in deploying the E2E training methodology.

In response to these challenges, some researchers have begun exploring local learning as an alternative to the conventional E2E training methodology [14], [15], [16]. This approach divides the deep network into distinct modules, employing gradient isolation to facilitate the independent training of each module under local supervision [17]. Local learning conducts parameter updates within its respective modules, obviating the need to retain all intermediate activation values as necessitated by E2E, thereby markedly reducing GPU memory requirements during training [6]. Concurrently, this method enhances training efficiency [15] and enables model parallelization [18]. Moreover, local learning’s emphasis on local error signals aligns more closely with the principles of biological plausibility [19], [20]. Nevertheless, local learning overly focuses on the local features of the model, coupled with a lack of inter-module interaction, can result in global performance that does not measure up to E2E standards [11], [18]. Although a large number of studies have been conducted to improve the performance degradation problem in Local Learning to a certain extent [6], [11], [15], it is still far from

the performance of E2E methods. It will greatly limit the role of Local Learning as an alternative to E2E in some accuracy-seeking tasks. Therefore, a primary objective within the local learning domain is to preserve as many global features as possible to bolster performance. Additionally, achieving a balance between the efficiency of GPU memory usage and the global performance outcome is imperative, which would render local learning a more universally viable alternative to E2E.

In this work, we introduce MLAAN, a novel supervised local learning approach, as illustrated in Figure 2. It is designed to facilitate enhanced inter-module communication and address the issue of model myopia, thereby significantly elevating the performance of supervised local learning to achieve state-of-the-art results. MLAAN employs a dual architecture so that three neighboring modules share weights. The independent auxiliary network in the architecture is used to acquire local features by generating unique losses, while the cascade auxiliary network is used to facilitate sharing between modules to acquire global features. The standalone and cascade levels complement each other, thus enabling to learn both global and local features for effective supervision and coordination. Additionally, MLAAN incorporates a leap augmented module, which serves to counteract the reduced learning capacity often associated with weaker supervision. This module provides strategic positioning between the primary and secondary networks within each gradient-isolated network module, thereby enhancing the exchange of information between current and later local units. The synergy between the dual architecture and the leap augmented module culminates in a comprehensive enhancement of network performance. The principal contributions of this research are delineated as follows.

- We propose a new method called MLAAN that successfully addresses the above mentioned shortcomings of traditional local learning and offers hope for the development of deep learning algorithms that are more efficient and biocompatible than traditional E2E training methods.
- MLAAN is a plug-and-play generalised method with excellent generalisation to all types of supervised local learning methods.
- MLAAN combined with existing supervised local learning methods can improve greatly its performance, making it perform better than E2E on CIFAR-10 [21], SVHN [22], STL-10 [23] and ImageNet [24] datasets while saving GPU memory, thus reaching the current state of the art.

II. RELATED WORK

A. Alternatives of backpropagation

Owing to challenges such as high GPU memory consumption, diminished training efficiency, barriers to model parallelization, and suboptimal biological plausibility, the advancement of traditional E2E learning approaches has been significantly constrained. In light of these issues, researchers have recently shifted their focus toward developing alternative

training strategies for E2E models [11]. To avoid backpropagation of the model and thus solve the problems of high memory consumption and low training efficiency, some scholars have proposed the target propagation method that directly propagates the target values by generating autoencoders [25], [26], [27] and the feedback alignment method that directly updates the weights of each layer by propagating the global loss values directly to each hidden layer [28], [29]. Decoupling neural interfaces for generating synthetic gradients by designing auxiliary networks [30] is also one of the effective ways. Meanwhile, training neural networks using feature replay [31] and decoupled parallel backpropagation algorithms with convergence guarantees [32] have been proposed to further address the problem of hindering the parallelisation of models based on the above methods. In addition, some scholars have proposed the use of forward gradient learning to completely replace backpropagation [33], [34]. However, the majority of these methodologies continue to depend on global loss values, which are less biologically plausible compared to local learning approaches. To date, these methods have not successfully tackled the challenges presented by large-scale datasets such as ImageNet [24].

B. Self-supervised local learning

Local learning is considered a promising alternative to traditional E2E as a new interactive training method due to its advantages of low training cost, high training efficiency, allowing model parallelization, and being more biologically compatible [15]. However, its lack of local inter-module interaction and thus poor global performance has seriously hampered the development of local learning domains [17].

Based on the above, scholars started to try to use different methods to improve the global performance of local learning. A group of scholars chose to use self-supervised loss to preserve as many features as possible during local module propagation [35]. For example, S. A. Siddiqui et al [36] used the Barlow Twins loss for Blockwise Self-Supervised Learning; Y. Xiong et al [37] designed SimCLR loss for Local Contrastive Learning; Sindy et al [38] applied Comparative Predictive Coding loss to reduce feature loss in Greedy InfoMax during propagation. Although the above methods show better performance when the number of blocks into which the deep network is divided is small, they do not perform well when the deep network is divided into a large number of blocks. And then the method proposed by Adrien et al [39] that combines Hebbian learning with local learning solves the above problem, but it runs into challenges on large datasets such as ImageNet [24].

C. Supervised local learning

In this context, some scholars began to turn their goals to supervised local learning. On the one hand, scholars have worked on finding suitable local losses to effectively improve the ability of local modules to retain global information. For example, Y. Wang et al [6] designed reconstruction loss and cross-entropy loss for each hidden layer in the InfoPro network, thus forcing the hidden layer to retain as many important

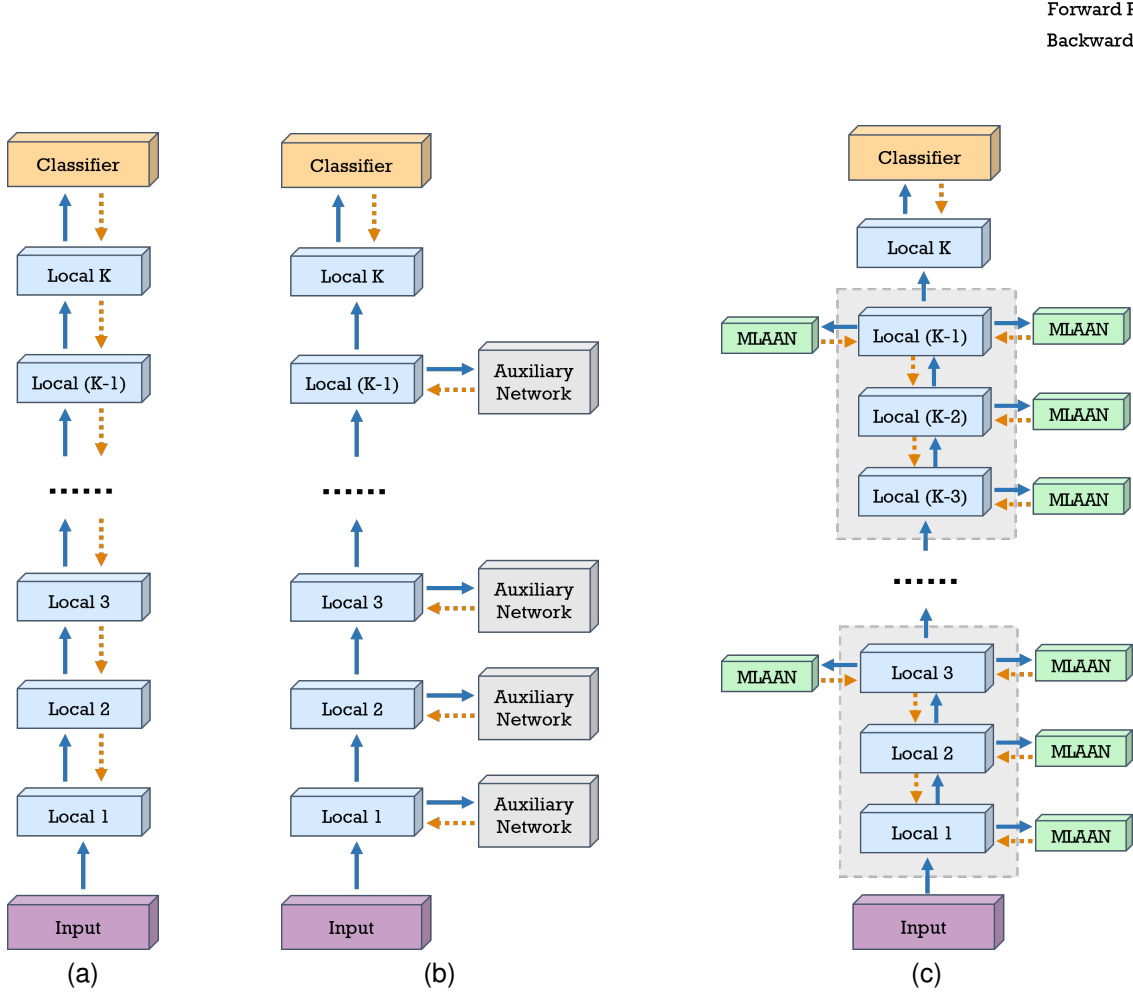


Fig. 2. The MLAAN overall architecture. (a) E2E training. (b) Other supervised local learning. (c) Our method.

input features as possible. On the other hand, scholars are making advanced auxiliary networks to improve the mutual synergy between different layers. For example, E. Belilov et al [11] proposed the algorithmic structure of DGL. It takes a different approach by considering the speed of auxiliary networks in relation to their corresponding primary network modules. The goal of dramatically improving local learning performance is achieved.

The emergence of methods such as InfoPro [6] and DGL [11] overcomes the challenges of local learning on large datasets such as ImageNet [24] and improves the performance of local learning to a greater extent. However, the lack of information exchange between the modules of their own gradient isolation causes their performance to still be far from E2E. How to enhance the information exchange between modules so that the performance of local learning approaches or even exceeds that of E2E is still the key issue we have to face. It is in this context that this paper is dedicated to designing a new method to facilitate enhanced inter-module communication and address the issue of model myopia. The goal is to significantly elevate the performance of supervised local learning, and enable us to implement more advanced and complex training of large models on arithmetic-limited

platforms.

III. METHOD

A. Preparations

To commence, we provide an overview of the conventional end-to-end (E2E) BP-supervised learning paradigm and the back-propagation mechanism for contextual clarity. Assume that x and y denote a data sample and its corresponding true label, respectively. We propose f_{θ} as a neural network equipped with the parameter θ , and its forward computation is denoted as $f(\cdot)$. This deep network can be divided into multiple local modules.

During forward propagation, the output of the j -th local module is used as the input of the subsequent $(j+1)$ -th local module, where $x_{j+1} = f_{\theta_j}(x_j)$. The loss function $\mathcal{L}(\hat{y}, y)$ is computed based on the comparison between the last local module's output and its true label. The computed gradient is then back-propagated iteratively to the previous modules.

Existing supervised local learning methods [40], [41], [42] aim to enhance learning performance by dividing the network into modules and designing auxiliary networks for each local module. The output of a local module is directed to its corresponding auxiliary network to generate local monitoring

signals $\hat{y}_j = g_{\gamma_j}(x_{j+1})$, where $g_{\gamma_j}(\cdot)$ represents the auxiliary network updating function.

In this configuration, the updates are made based on the following equations:

$$\gamma_j \leftarrow \gamma_j - \eta_\alpha \times \nabla_{\gamma_j} \mathcal{L}(\hat{y}_j, y) \quad (1)$$

$$\theta_j \leftarrow \theta_j - \eta_\ell \times \nabla_{\theta_j} \mathcal{L}(\hat{y}_j, y) \quad (2)$$

where γ_j, θ_j means updated parameters of the auxiliary networks and the local modules, η_α, η_ℓ denote the learning rate of them, respectively. The application of the auxiliary network empowers each module gradient to be isolated, thus enabling updates via local supervision instead of global backpropagation.

B. Multilaminar Local Modules

Current supervised local learning methods have certain limitations. These methods rely on auxiliary networks to update each gradient-isolated local module independently, which hinders information sharing and interaction between local modules. This lack of inter-module coordination can result in suboptimal outcomes. To address these issues, we propose multilaminar local modules to facilitate inter-module communication.

In our multilayer local supervision module, we divide the entire network into two levels of local modules: cascaded modules and independent modules. Each local module functions as an independent module unit, while multiple adjacent local modules form a cascaded module. The auxiliary network is connected to each independent or cascaded module to enable effective supervision and coordination.

We assume that each cascaded module computes $k(k > 1)$ local modules and the intersects with local modules in adjacent cascades. For example, the first cascaded module consists of $f_{\theta_1}, \dots, f_{\theta_k}$, the second cascaded module consists of $f_{\theta_2}, \dots, f_{\theta_{k+1}}$, and so on. For the j -th local module, denoted as f_{θ_j} , it receives a signal from an independent auxiliary network g_{γ_j} and k cascaded auxiliary network $h_{\beta_i}, \dots, h_{\beta_{i+k-1}}$, where $i = j - k + 1$. The output of the j -th local module within independent auxiliary network is represented as $\hat{y}_j = g_{\gamma_j}(x_{j+1})$. The i -th cascaded auxiliary network denotes the $(i + k - 1)$ -th local module, i.e., the last module of the i -th cascaded, $\hat{y}_i = h_{\beta_i}(x_{i+k})$. In this framework, local supervision of a particular local module occurs $k + 1$ times, once from the $\mathcal{L}(\hat{y}_j, y)$, and k times from $\mathcal{L}(\hat{y}_i, y), \dots, \mathcal{L}(\hat{y}_{i+k-1}, y)$.

The updated rules can be summarized as follows:

$$\gamma_j \leftarrow \gamma_j - \eta_d \times \nabla_{\gamma_j} \mathcal{L}(\hat{y}_j, y) \quad (3)$$

$$\beta_j \leftarrow \beta_j - \eta_c \times \nabla_{\beta_j} \mathcal{L}(\hat{y}_i, y) \quad (4)$$

$$\theta_j \leftarrow \theta_j - \eta_d \times \nabla_{\theta_j} \mathcal{L}(\hat{y}_j, y) - \sum_{n=i}^{i+k-1} (\eta_c \times \nabla_{\theta_j} \mathcal{L}(\hat{y}_n, y)) \quad (5)$$

where η_d, η_c are the learning rates of the independent and cascaded auxiliary networks, respectively. In equation (5), the initial gradient descent term represents the supervision

from the independent auxiliary network, while the latter term corresponds to the supervision from the.

During practical implementation, we typically set $k = 3$, indicating that the influence of the cascaded auxiliary network extends to three consecutive local modules. This choice strikes a balance between computational efficiency and the risk of overfitting. Setting k to a larger value would make the training method closer to BP, which could significantly increase GPU memory usage. Moreover, a larger value of k would subject the same local modules to local supervision more frequently, thereby raising the likelihood of overfitting.

C. Leap Augmented Modules

In traditional supervised local learning methods, the training of each local module with a simple auxiliary network often leads to insufficient supervision of the hidden layers, resulting in subpar learning outcomes. The remarkable performance of E2E training can be attributed to the fact that the entire network updates its parameters based on a global error signal. Consequently, the interaction of information between neural network layers plays a crucial role in the overall performance of the model.

As the network depth increases, the acquired information becomes more semantic, and the ability to comprehend high-level information improves. In contrast, a shallow network can only capture low-level information such as colors and textures, making the subsequent network layers even more critical. To enhance the learning capacity of the hidden layers, it is beneficial to allow each gradient-isolated local module to access information from subsequent deeper modules. This arrangement facilitates the exchange of information between the modules, thereby improving the overall learning process.

To address the issue of information sharing between local modules, we introduce generic leap augmented modules. These modules are strategically positioned between the main and auxiliary networks within each gradient-isolated network module. Their purpose is to enhance the exchange of information between the current local module and subsequent local modules, thereby promoting improved learning outcomes.

As shown in Figure 3, in the design process of leap augmented modules, for the j -th local module f_{θ_j} , its auxiliary network is denoted as g_{γ_j} . We assume that the j -th local module f_{θ_j} is expected to receive information from $p(p \geq 1)$ hidden layers, distributed across the early, intermediate, and deeper layers of the subsequent local modules. To facilitate information exchange with the subsequent local modules, we perform a deepcopy operation twice: $\varphi'_{j+l}, \varphi''_{j+l} = \text{deepcopy}(m^{j+l})$, where m^{j+l} represents the hidden layer extracted in the $(j + l)$ -th local module. The first copy, φ'_{j+l} , is updated by g_{γ_j} , while the second copy, φ''_{j+l} , is updated by Exponential Moving Average(EMA). The update rules are as follows, where r is a hyperparameter, and λ_{EMA_j} is the updated parameter of EMA.

$$\gamma_j \leftarrow \gamma_j - \eta_d \times \nabla_{\gamma_j} \mathcal{L}(\hat{y}_j, y) \quad (6)$$

$$\lambda_{EMA_j} \leftarrow r \times \lambda_{EMA_j} + (1 - r) \times \gamma_j \quad (7)$$

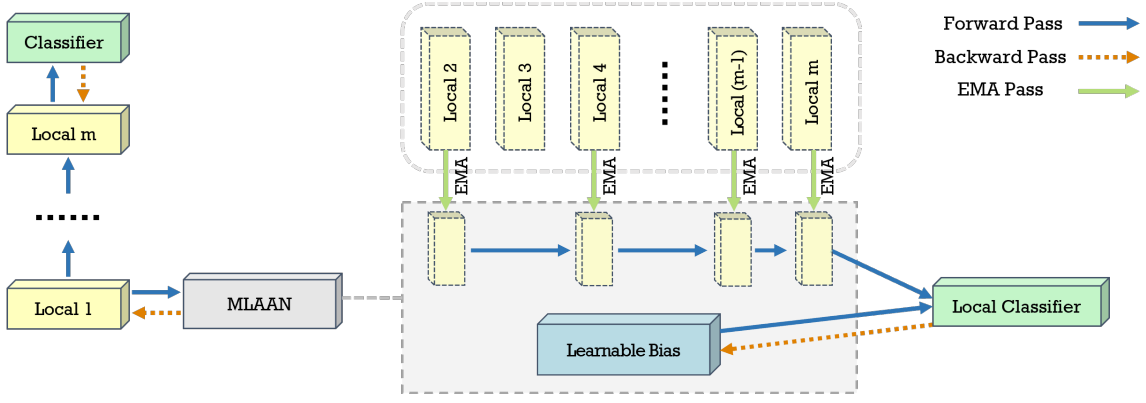


Fig. 3. The Leap Augmented Modules architecture. As the proximity to the early blocks increases, the utilization of auxiliary layers employing EMA decreases.

D. Multilaminar Leap Augmented Locally Supervised Learning

Multilaminar Local Modules and Leap Augmented Modules each possess distinct characteristics. The utilization of Multilaminar Local Modules significantly enhances the classification capability. However, it originates from a global objective, leading to limited learning ability for local features. On the other hand, Leap Augmented Modules exhibit the opposite behavior. While they may have slightly lower classification capability, their advantage lies in their ability to better capture the internal variations of local features. Based on the characteristics of the above two approaches for global information exchange and local learning enhancement, we fuse the two approaches to make it a Scaling Supervised Local Learning with Multilaminar Leap Augmented Auxiliary Network (MLAAN).

In the last local module, denoted as s , within a given cascaded module, f_{θ_s} receives $k+1$ local supervisions. Among these, k from $\mathcal{L}(\hat{y}_i, y), \dots, \mathcal{L}(\hat{y}_{i+k-1}, y)$, while one comes from $\mathcal{L}(\hat{y}_s, y)$, where $\hat{y}_s = g_{\gamma_s}(x_{s+1})$. Upon incorporating the Leap Augmented Modules, the reinforcement layers are integrated into the cascaded auxiliary networks and updated using λ_{EMAS} . The overall update rules for MLAAN are described as follows:

$$\gamma_s \leftarrow \gamma_s - \eta_d \times \nabla_{\gamma_s} \mathcal{L}(\hat{y}_s, y) \quad (8)$$

$$\lambda_{EMAS} \leftarrow r \times \lambda_{EMAS} + (1-r) \times \gamma_s \quad (9)$$

$$\theta_s \leftarrow \theta_s - \eta_d \times \nabla_{\theta_s} \mathcal{L}(\hat{y}_s, y) \quad (10)$$

$$- \{r \times \lambda_{EMAS} + (1-r) \times \eta_d \times \nabla_{\theta_s} \mathcal{L}(\hat{y}_s, y)\} \quad (11)$$

$$\theta_s \leftarrow \theta_s - r \times \lambda_{EMAS} - (2-r) \times \eta_d \times \nabla_{\theta_s} \mathcal{L}(\hat{y}_s, y) \quad (11)$$

Indeed, MLAAN has demonstrated excellent performance in various tasks. The design of multilaminar local modules and their framework allows for learning at different levels of granularity. The independent modules focus on extracting local features, while cascaded modules capture global features through the interconnectivity among their local modules. This combination significantly enhances the overall network performance by effectively leveraging both local and global information.

Within the leap augmented modules, φ'_j utilizes the network structure of the hidden layers in subsequent local modules

without sharing gradients with them. Its main function is to support the learning capability of the hidden layers within each local network module. φ'_j focuses on enhancing intra-local module learning, while φ''_j ensures inter-local module communication. This harmonious interplay between φ'_j and φ''_j leads to substantial improvement in the performance of supervised local learning methods.

Furthermore, the MLAAN framework exhibits robust generalization capabilities. It seamlessly integrates with existing supervised local learning methods, enhancing its practicality and generality.

IV. EXPERIMENT

A. Datasets

In this section, we provide a brief introduction to the four image classification datasets that we utilized, as well as the data augmentation methods employed.

CIFAR-10 [21] dataset contains 60,000, 32×32 color images, divided into 10 classes, with 6,000 images per class. These classes include airplanes, cars, birds, cats, deer, dogs, frogs, horses, ships, and trucks. The dataset is divided into 50,000 training images and 10,000 test images.

SVHN [22] is a real-world image dataset used for developing machine learning and object recognition algorithms, especially for recognizing digits in visual objects. It is derived from Google Street View data and contains over 600,000 images of digits, covering 10 classes (0-9). Each image is a 32×32 pixel color image.

STL-10 [23] dataset is designed to evaluate unsupervised feature learning and self-learning algorithms. It is inspired by the CIFAR-10 dataset but has some changes. It includes 10 classes, each with 500 training images and 800 test images. All images are 96×96 color images. In addition, an unlabeled dataset is provided, containing 100,000 additional images.

ImageNet [24] is a large-scale visual database composed of over 10 million high-resolution images with detailed labels. These images cover more than 20,000 categories, with the number of images per category ranging from a few hundred to tens of thousands. The goal of ImageNet is to provide researchers with an easily accessible, large-scale image database to assist them in their research in computer vision and other fields.

B. Experimental Setup

We conduct experiments using ResNet [43] network architectures of varying depths on four widely used datasets: CIFAR-10 [21], SVHN [22], STL-10 [23], and ImageNet [24].

In our research, we integrate MLAAN with two advanced methods, DGL [40] and InfoPro [42], to assess its performance. Initially, each network is divided into K local modules, with approximately equal numbers of layers and corresponding auxiliary network operations. The K represents the number of gradient-isolated local modules that need to be trained in each epoch. An increase in the K leads to a reduction in GPU memory usage, but concurrently, it can result in a decrease in performance. Therefore, comparing performance at the same K is fair.

During the training process, our proposed MLAAN is applied to the first $(K-1)$ modules, while the final module is directly connected to global pooling and fully connected layers to generate classification results. Subsequently, this configuration is compared against global backpropagation (BP) [44] and the original supervised local learning methods, ensuring the transfer of confounding variables for a scientifically and methodologically designed experiment.

C. Implement Detail

In our experiments, we utilized ResNet-32 [43] and ResNet-110 [43] as the backbone networks on the CIFAR-10 [21], SVHN [22], and STL-10 [23] datasets. The SGD optimizer [45] with Nesterov momentum [46] set at 0.9 and an L2 weight decay factor of $1e-4$ is employed. When ResNet-32 [43] is used as the backbone network, we divide it into 16 modules. Similarly, for ResNet-110 [43], it is segmented into 55 modules. Each local module possesses its own set of parameters, including an accompanying auxiliary network.

Furthermore, different hyperparameters are employed for each dataset. For CIFAR-10 [21] and SVHN [22], we set the batch size to 1024, while for STL-10 [23], it is set to 128. The training process lasts for 400 epochs, starting with an initial learning rate of 0.8 for CIFAR-10 [21] and SVHN [22], and 0.1 for STL-10 [23], following a cosine annealing scheduler [47]. In our ImageNet [24] experiments, we utilize different training settings for various network structures. Specifically, for ResNet-34 [43], ResNet-101 [43], and ResNet-152 [43], we train them for 150 epochs with an initial learning rate of 0.05 and a batch size of 128. We maintain consistency with the previously described configurations for CIFAR-10 [21].

D. Comparison with the SOTA results

1) *Results on various image classification benchmarks:* We initially conduct experiments on the CIFAR-10 [21], SVHN [22] and STL-10 [23] datasets to evaluate the performance of MLAAN. The experimental results are summarized in Table I. It is evident from the results that our proposed MLAAN exhibits substantial improvements across various methods and datasets. Not only does it surpass the performance of previous methods, but more importantly, it consistently outperforms the End-to-End (E2E) approaches.

The experimental results obtained on the CIFAR-10 [21] dataset indicate that our proposed method, MLAAN, exhibits more pronounced benefits as the network is divided into a larger number of local modules. For instance, in the case of ResNet-32 ($k=16$) [43], where each hidden layer is treated as a local module, the test error is reduced by 54% without attaching either DGL [40] or InfoPro [42] methods. Using MLAAN significantly reduces the test error compared to DGL [40] and InfoPro [42] methods. Specifically, the test errors are reduced from 14.08 and 12.93 to 6.36 and 6.37, respectively. This signifies a substantial performance improvement of 55% and 51% over the BP [44] baseline.

Furthermore, even with deeper network architectures like ResNet-110 ($k=55$) [43], MLAAN continues to enhance the performance of both DGL [40] and InfoPro [42] methods. It results in remarkable improvements of 61% and 56% respectively. These experimental findings demonstrate the versatility of MLAAN, as its performance enhancement is not limited by network depth or the specific methodology employed.

As the experiments were extended to include other datasets, the MLAAN approach consistently demonstrated superior performance compared to the baseline method, BP [44]. Specifically, on the STL-10 [23] dataset, MLAAN achieved significant improvements of over 30% and 34% for the DGL [40] and InfoPro [42], respectively. Similarly, on the SVHN [22] dataset, MLAAN results in even more remarkable enhancements, with performance gains exceeding 42% and 49% across different evaluation metrics.

These experimental results serve to validate the remarkable effectiveness of the MLAAN approach in improving the performance of deep learning models. Despite considering each hidden layer as a locally isolated module for gradient propagation, MLAAN demonstrates its ability to substantially bridge the performance gap that exists. This underscores the potential of MLAAN as a powerful technique for enhancing the training process and optimizing the performance of deep learning models across various datasets.

2) *Results on ImageNet:* We conduct experiments to evaluate the performance of MLAAN on the highly challenging large-scale dataset, ImageNet [24]. In these experiments, we utilize ResNet-34 [43] as the backbone network and divide it into 17 local modules, as described in Table II. By incorporating MLAAN into the training process, we observe a notable performance improvement. Specifically, the Top1-Error and Top5-Error metrics both decreased by 0.3%, resulting in MLAAN achieving performance that is comparable to the baseline method, BP [44].

We further extend experiments using ResNet-101 [43] and ResNet-152 [43] as the backbone networks, dividing them into 34 and 51 local modules, respectively. The results, as presented in Table II, demonstrate the effectiveness of MLAAN in improving the performance of these deeper networks compared to the baseline method, BP [44].

Specifically, when MLAAN is introduced, ResNet-101 [43] exhibits reductions in Top1-Error and Top5-Error by 0.09% and 0.7%, respectively. Similarly, by incorporating MLAAN into the training process of ResNet-152 [43], we observe reductions in Top1-Error and Top5-Error by 0.2% and 0.5%

TABLE I
COMPARISON OF SUPERVISED LOCAL LEARNING METHODS AND BP ON IMAGE CLASSIFICATION DATASETS. THE AVERAGED TEST ERRORS ARE REPORTED FROM THREE INDEPENDENT TRIALS. THE * MEANS THE ADDITION OF OUR MLAAN.

Dataset	Method	ResNet-32		ResNet-110	
		K=8(Test Error)	K=16(Test Error)	K=32(Test Error)	K=55(Test Error)
CIFAR-10 (BP(ResNet-32)=6.37, BP(ResNet-110)=5.42)	DGL	11.63	14.08	12.51	14.45
	DGL*	6.25±0.12(↓5.26-5.50)	6.36±0.15(↓7.57-7.87)	5.38±0.27(↓6.86-7.40)	5.42±0.52(↓8.51-9.03)
	InfoPro	11.51	12.93	12.26	13.22
	InfoPro*	6.37±0.50(↓4.64-5.14)	6.37±0.35(↓6.21-6.91)	5.41±0.49(↓6.36-7.34)	5.60±0.55(↓7.07-7.62)
STL-10 (BP(ResNet-32)=19.35, BP(ResNet-110)=19.67)	DGL	25.05	27.14	25.67	28.16
	DGL*	19.35±0.51(↓5.19-6.21)	19.02±0.11(↓8.01-8.23)	19.54±0.34(↓5.79-6.47)	19.66±0.55(↓7.95-8.50)
	InfoPro	27.32	29.28	28.58	29.20
	InfoPro*	19.21±0.19(↓7.92-8.30)	19.21±0.12(↓9.95-10.19)	19.51±0.16(↓8.91-9.23)	19.24±0.21(↓9.75-10.17)
SVHN (BP(ResNet-32)=2.99, BP(ResNet-110)=2.92)	DGL	4.83	5.05	5.12	5.36
	DGL*	2.79±0.12(↓1.92-2.16)	2.73±0.19(↓2.13-2.51)	2.78±0.22(↓2.12-2.56)	2.90±0.14(↓2.32-2.46)
	InfoPro	5.61	5.97	5.89	6.11
	InfoPro*	2.97±0.18(↓2.46-2.82)	2.95±0.2(↓2.82-3.02)	2.87±0.32(↓2.70-3.34)	2.90±0.42(↓2.79-3.21)
	DGL	2.85±0.22	2.82±0.38	2.79±0.31	2.89±0.31
	DGL*				
	InfoPro				
	InfoPro*				

TABLE II
RESULTS ON THE VALIDATION SET OF IMAGENET

Backbone	Method	Top1-Error	Top5-Error
ResNet-34 (K=17)	BP	25.38	7.90
	MLAAN	25.31(↓0.07)	7.88(↓0.02)
ResNet-101 (K=34)	BP	22.03	5.93
	MLAAN	21.69(↓0.34)	5.72(↓0.21)
ResNet-152 (K=51)	BP	21.60	5.92
	MLAAN	21.34(↓0.26)	5.74(↓0.18)

compared to BP. Notably, the improvement in Top5-Error is particularly significant.

These substantial performance gains enable the networks to surpass the performance of BP, even when divided into a larger number of local modules (34 and 51 for ResNet-101 [43] and ResNet-152 [43], respectively). These findings reinforce the effectiveness of MLAAN in improving the accuracy and robustness of deep learning models, especially in scenarios involving complex and deep architectures.

3) *Training-Accuracy Curve Analysis*: To illustrate the impact of our proposed method on training performance, we have compared a comparative analysis between the original method and the method enhanced with MLAAN. We visualized the accuracy-epoch curves and the results are presented in Figure 4. Our proposed MLAAN consistently outperforms the original model across different backbones. Notably, significant improvements are observed in terms of both convergence speed and accuracy.

The curve of the original method exhibits considerable fluctuations, particularly in the early stages of training. There are noticeable discrepancies in accuracy between adjacent epochs, which indicates unpredictability and potential limitations when making robust predictions and adapting to different data patterns. In contrast, our method effectively addresses this issue by mitigating instability and significantly enhancing both accuracy and convergence speed. Consequently, the training time is shortened and overall efficiency is improved.

4) *Memory Consumption*: Due to the characteristic of gradients not propagating between local modules, local learning is capable of significantly reducing GPU memory usage during

TABLE III
COMPARISON OF GPU MEMORY USAGE BETWEEN BP AND OTHER METHODS WITH MLAAN ON THE CIFAR-10 AND IMAGENET DATASETS.

Dataset	Network	Method	GPU Memory(GB)
CIFAR-10	ResNet-32 (K=16)	BP	3.37G
		MLAAN	2.62G(↓22.3%)
	ResNet-110 (K=55)	BP	9.26G
		MLAAN	2.76G(↓70.2%)
ImageNet	ResNet-34 (K=17)	BP	10.74G
		MLAAN	9.09G(↓15.4%)
	ResNet-101 (K=34)	BP	20.64G
		MLAAN	17.93G(↓13.1%)
	ResNet-152 (K=51)	BP	26.29G
		MLAAN	23.01G(↓12.5%)

the training process. We investigate the GPU memory usage of both BP and MLAAN on the CIFAR-10 [21] and ImageNet [24] datasets. The comparative results can be found in Table III.

On the CIFAR-10 [21] dataset, we observe substantial reductions in GPU memory usage when combining MLAAN with DGL [40] and InfoPro [42]. Specifically, when applied to ResNet-32 (k=16) [43], the GPU memory usage decreases by 22.3% compared to BP [44]. This reduction becomes even more significant when extending the experiments to deeper networks like ResNet-110 (k=55) [43], with a remarkable reduction of 70.2% in GPU memory usage.

In the GPU memory usage tests conducted on the ImageNet [24] dataset, the incorporation of MLAAN yields notable reductions in GPU memory usage across different backbone networks. ResNet-34 [43], ResNet-101 [43], and ResNet-152 [43] show reductions of 15.4%, 1.7%, and 12.5%, respectively, when compared to BP [44]. This signifies that we have achieved higher performance while utilizing less GPU memory than BP [44].

E. Ablation Study

1) *Comparison between Multilaminar Local Modules, Leap Augmented Modules, and MLAAN*: To further elucidate the contributions of Multilaminar Local Modules and Leap Augmented Modules to MLAAN in the context of feature learning,

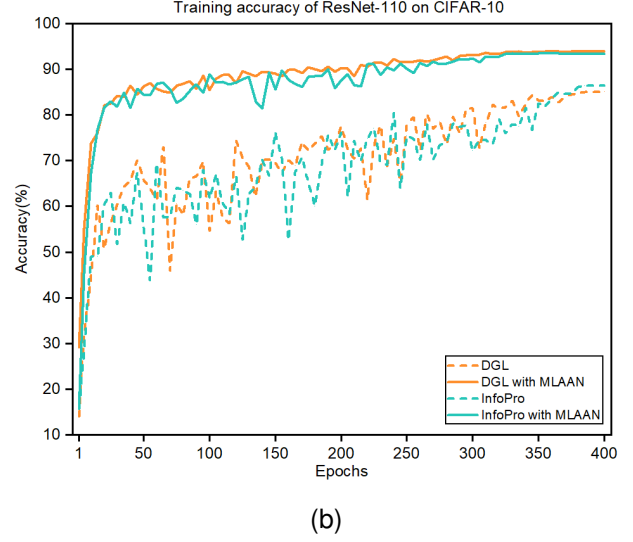
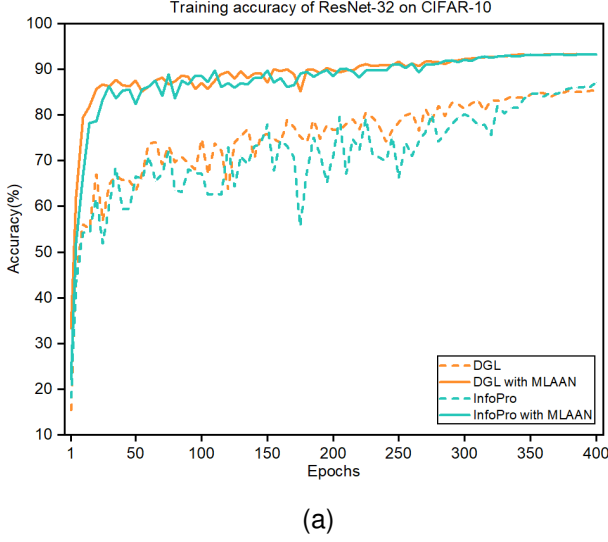


Fig. 4. Training-Accuracy curves, the figure on the left is obtained using ResNet-32 (K=16) on the CIFAR-10 dataset, while the figure on the right are obtained using ResNet-110 (K=55) on the CIFAR-10 dataset.

TABLE IV
RESULTS FROM EXPERIMENTS CONDUCTED ON THE CIFAR-10 DATASET.
MLM AND LAM MEAN MULTILAMINAR LOCAL MODULES AND LEAP
AUGMENTED MODULES RESPECTIVELY.

MLM	LAM	Test Error
×	×	14.08
✓	×	8.46(↓5.62)
×	✓	7.64(↓6.44)
✓	✓	6.36(↓7.28)

we conduct experiments using ResNet-32 (K=16) [43] as the backbone network, DGL [40] as the baseline, and experiments are performed with Multilaminar Local Modules, Leap Augmented Modules, and MLAAN. The experimental results are summarized in Table IV.

From the results presented in the table, it is evident that in the absence of Multilaminar Local Modules and Leap Augmented Modules, the Test Error is significantly higher at 14.08. Upon incorporating Multilaminar Local Modules individually, there is a respective decrease in Test Error of 5.62 and 6.44. Notably, when both modules are combined, the Test Error drops even further to 6.80, representing a substantial decrease of 7.28. These findings provide compelling evidence of the significant contributions made by Multilaminar Local Modules and Leap Augmented Modules, highlighting the remarkable performance achieved by MLAAN through their integration.

2) *Comparative Analysis of Unfair Epochs*: Undeniably, the utilization of MLAAN introduces additional Wall Time, prompting us to conduct a comparative analysis of unfair epochs. The findings of this analysis can be observed in Table V. When using DGL [40] as the baseline, after incorporating MLAAN, it only takes 300 epochs to reduce the Test Error by 45% for a Backbone of ResNet-32 (K=16) [43] and 52% for ResNet-110 (K=55) [43].

3) *Comparison of Features in Different Methods*: In our

TABLE V
THE DATA IN THE TABLE REPRESENT THE TEST ERROR.

Dataset	Method	ResNet-32 (K=16)	ResNet-110 (K=55)
CIFAR-10	DGL(Epochs=400)	14.08	14.45
	DGL*(Epochs=300)	7.79(↓6.29)	6.98(↓7.47)

research, we aim to demonstrate the competitive performance of our proposed MLAAN in comparison to BP [44]. To showcase the advanced capabilities of MLAAN, we conduct feature map analyses on different configurations, including DGL [40], DGL with Multilaminar Local Modules, DGL with Leap Augmented Modules, and DGL with MLAAN. In feature maps, a deeper shade of red indicates a higher level of attention concentration. The resulting figures detailing these feature maps can be found in Figure 5. From left to right are four feature maps representing four methods: DGL, DGL with Leap Augmented Modules, DGL with Multilaminar Local Modules and DGL with MLAAN.

Upon analyzing the feature maps, we observe that (a) is concentrated in specific regions, indicating the presence of significant information within those areas. Conversely, after the fusion of (b) and (c), (d) captures more comprehensive global features, including localized edge features.

For (a), the lack of communication between successive modules results in suboptimal feature learning performance. It primarily focuses on specific regions, neglecting global semantic features and leading to poor classification ability in the early blocks. In contrast, our approach provides greater granularity, enabling the observation of more global semantic features. However, it partially overlooks localized features, suggesting potential for improving the classification ability on challenging samples. Thus, under the supervised local learning framework, our MLAAN compensates for the shortcomings of other methods.

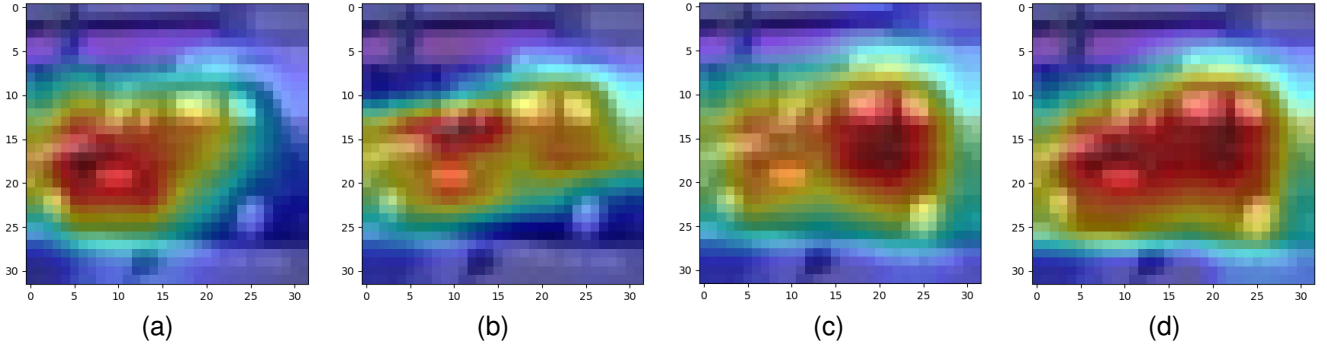


Fig. 5. Visualization of channel feature maps. (a) Feature Map of DGL. (b) Feature Map of DGL with Leap Augmented Modules. (c) Feature Map of DGL with Multilaminar Local Modules. (d) Feature Map of DGL with MLAAN.

4) *Decoupled Layer Accuracy Analysis*: We have demonstrated that MLAAN can achieve comparable accuracy to BP [44] across different network architectures. To further discuss how our method strengthens network performance, we freeze the parameters of the main network and train a linear classifier for each gradient-isolated hidden layer to determine the classification accuracy at each layer. The results are shown in Figure 6, where we use DGL [40] as the baseline for comparison.

In our approach, we acknowledge that high classification accuracy in the early layers may not necessarily be beneficial from a global perspective. If the early layers solely optimize local objectives, they may discard useful features that could be valuable for subsequent layers. This would result in less effective information being learned by the following layers and ultimately result in suboptimal performance of the network.

However, after incorporating MLAAN, the classification accuracy of the early layers notably decreases as they acquire more globally useful features, thereby strengthening the generalization ability of the subsequent layers. This result suggests that MLAAN alleviates the myopia problem often associated with supervised local learning methods. By allowing gradient-isolated local modules to simultaneously learn both global and local features, MLAAN enhances the overall performance and generalization ability of the network.

5) *Representation Similarity Analysis*: To further demonstrate the effectiveness of our method, we conduct Centered Kernel Alignment (CKA) [48] experiments. CKA is a similarity index that enables a quantitative comparison of the similarity between different neural network models at the same layer. Specifically, we use DGL [40] as the baseline and incorporate our MLAAN to calculate the CKA [48] similarity of each layer compared to BP [44], and then compute their mean values. The results of these experiments are presented in Figure 7.

We can observe that our method significantly improves the CKA similarity of DGL [40], particularly in the early layers. This improvement is crucial as higher CKA similarity in the early layers indicates that their learning patterns are closer to those of BP [44], implying that they are learning more features that are beneficial for the global objective. The poor performance of the original method is due to the

excessive focus of the early layers on local optimization objectives, resulting in significant differences in the learning approach compared to BP and leading to a decrease in overall performance.

By implementing the CKA experiments, we have successfully demonstrated that our method effectively addresses the lack of internal information exchange and shortsightedness commonly observed in current supervised local learning methods. By strengthening the network’s global perspective, our method consistently leads to performance improvements.

F. Generalization Study

TABLE VI
GENERALIZATION STUDY. CHECKPOINTS ARE TRAINED ON THE CIFAR-10 DATASET AND TESTED ON THE STL-10 DATASET. THE DATA IN THE TABLE REPRESENTS THE TEST ACCURACY.

Method	ResNet-32(K=16)	ResNet-110(K=55)
BP	35.98	36.78
DGL	31.95	33.16
DGL*	37.65	40.26

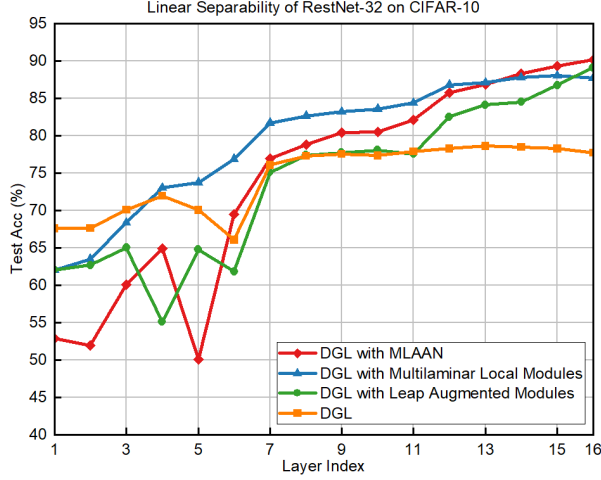
In this section, we aim to investigate the generalization performance of our proposed MLAAN method. To evaluate its effectiveness, we utilize the checkpoints trained on the CIFAR-10 [21] and test them on the STL-10 [23], taking inspiration from previous work [49].

As shown in Table VI, we observe a notable disparity in the generalization abilities of DGL [40] and BP [44]. However, with the incorporation of our MLAAN method, we witness a significant improvement in test accuracy, surpassing even that of BP [44]. These results indicate that MLAAN, by facilitating information interaction among local modules, effectively enhances the generalization ability of supervised local learning methods.

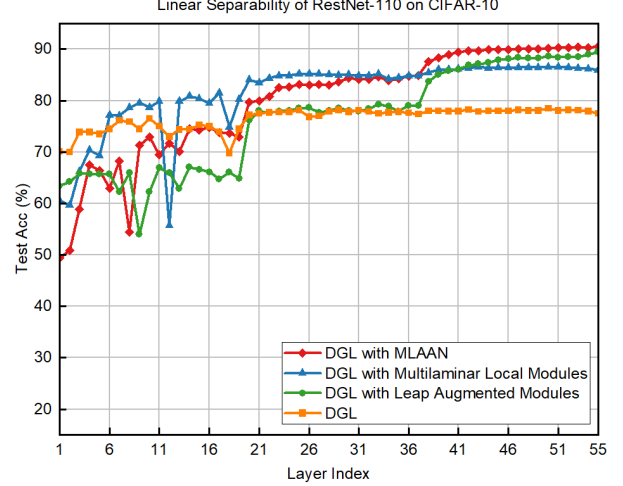
These findings emphasize the efficacy of our MLAAN method in improving the generalization capabilities of supervised local learning, ultimately leading to enhanced overall performance in the task of image classification.

V. CONCLUSION

This paper proposes a Scaling Supervised Local Learning with Multilaminar Leap Augmented Auxiliary Network

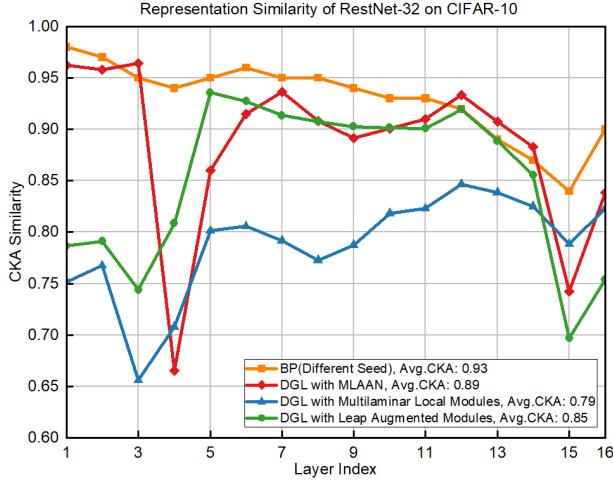


(a)

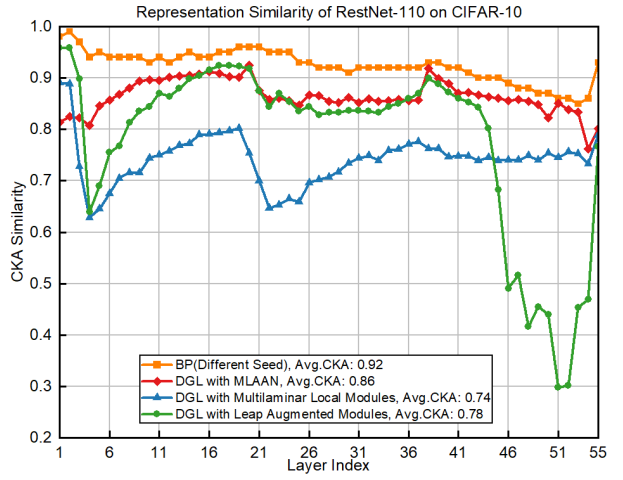


(b)

Fig. 6. Comparison of layer-wise linear separability across different learning rules on ResNet-32 and ResNet-110.



(a)



(b)

Fig. 7. Comparison of layer-wise representation similarity on ResNet-32 and ResNet-110.

(MLAAN). MLAAN employs a dual architecture so that three neighbouring modules share weights. The independent auxiliary network in the architecture is used to acquire local features by generating unique losses, while the cascade auxiliary network is used to facilitate sharing between modules to acquire global features. The standalone and cascade levels complement each other, thus enabling to learn both global and local features for effective supervision and coordination. Additionally, MLAAN incorporates a leap augmented module, which serves to counteract the reduced learning capacity often associated with weaker supervision. This module provides strategic positioning between the primary and secondary networks within each gradient-isolated network module, thereby enhancing the exchange of information between current and later local units. The synergy between the dual architecture

and the leap augmented module culminates in a comprehensive enhancement of network performance. The MLAAN method is a plug-and-play general-purpose method with excellent generalisation to all types of supervised local learning methods. The experimental evaluations conducted on four benchmark datasets, CIFAR-10, STL-10, SVHN, and ImageNet, demonstrate that the integration of MLAAN with existing supervised local learning methods significantly enhances the original methodologies, propelling them to achieve the current state-of-the-art. Of particular note, MLAAN enables local learning methods to comprehensively outperform end-to-end training approaches in terms of optimal performance while saving GPU memory. It can be anticipated that MLAAN will supplant E2E in real-world applications demanding high accuracy, particularly those requiring high-resolution data and ample

batch processing capabilities for training. Such applications encompass 2D/3D semantic segmentation and object detection in autonomous vehicles, tissue segmentation in medical imaging, and object recognition in remote sensing data. In conclusion, the MLAAN method significantly advances local learning by overcoming traditional performance degradation barriers. It establishes a foundation for local learning to potentially supplant E2E in tasks where precision is paramount. Meanwhile, it offers promising avenues for the development of deep learning algorithms that surpass the effectiveness and biocompatibility of conventional E2E training approaches.

REFERENCES

- [1] Y. Wang, C. Peng, and Y. Liu, "Mask-pose cascaded cnn for 2d hand pose estimation from single color image," *IEEE Transactions on Circuits and Systems for Video Technology*, vol. 29, no. 11, pp. 3258–3268, 2018.
- [2] J. Wang, H. Zhu, H. Liu, and Z. Ma, "Lossy point cloud geometry compression via end-to-end learning," *IEEE Transactions on Circuits and Systems for Video Technology*, vol. 31, no. 12, pp. 4909–4923, 2021.
- [3] H. Bao, P. Shu, H. Zhang, and X. Liu, "Siamese-based twin attention network for visual tracking," *IEEE Transactions on Circuits and Systems for Video Technology*, vol. 33, no. 2, pp. 847–860, 2022.
- [4] H. Li, M. Sun, J. Xiao, E. G. Lim, and Y. Zhao, "Fully and weakly supervised referring expression segmentation with end-to-end learning," *IEEE Transactions on Circuits and Systems for Video Technology*, 2023.
- [5] Y. He, X. Xu, J. Zhang, F. Shen, Y. Yang, and H. T. Shen, "Modeling two-stream correspondence for visual sound separation," *IEEE Transactions on Circuits and Systems for Video Technology*, vol. 32, no. 5, pp. 3291–3302, 2021.
- [6] Y. Wang, Z. Ni, S. Song, L. Yang, and G. Huang, "Revisiting locally supervised learning: an alternative to end-to-end training," *arXiv preprint arXiv:2101.10832*, 2021.
- [7] B. Wu, S. Nair, R. Martin-Martin, L. Fei-Fei, and C. Finn, "Greedy hierarchical variational autoencoders for large-scale video prediction," in *Proceedings of the IEEE/CVF Conference on Computer Vision and Pattern Recognition*, 2021, pp. 2318–2328.
- [8] M. Jaderberg, W. M. Czarnecki, S. Osindero, O. Vinyals, A. Graves, D. Silver, and K. Kavukcuoglu, "Decoupled neural interfaces using synthetic gradients," in *International conference on machine learning*. PMLR, 2017, pp. 1627–1635.
- [9] T. Salimans, J. Ho, X. Chen, S. Sidor, and I. Sutskever, "Evolution strategies as a scalable alternative to reinforcement learning," *arXiv preprint arXiv:1703.03864*, 2017.
- [10] S. Löwe, P. O'Connor, and B. Veeling, "Putting an end to end-to-end: Gradient-isolated learning of representations," *Advances in neural information processing systems*, vol. 32, 2019.
- [11] E. Belilovsky, M. Eickenberg, and E. Oyallon, "Decoupled greedy learning of cnns," in *International Conference on Machine Learning*. PMLR, 2020, pp. 736–745.
- [12] F. Crick, "The recent excitement about neural networks," *Nature*, vol. 337, no. 6203, pp. 129–132, 1989.
- [13] G. Shen, D. Zhao, and Y. Zeng, "Backpropagation with biologically plausible spatiotemporal adjustment for training deep spiking neural networks," *Patterns*, vol. 3, no. 6, 2022.
- [14] B. Illing, J. Ventura, G. Bellec, and W. Gerstner, "Local plasticity rules can learn deep representations using self-supervised contrastive predictions," *Advances in Neural Information Processing Systems*, vol. 34, pp. 30365–30379, 2021.
- [15] A. Nøkland and L. H. Eidnes, "Training neural networks with local error signals," in *International conference on machine learning*. PMLR, 2019, pp. 4839–4850.
- [16] Y. Xiong, M. Ren, and R. Urtasun, "Loco: Local contrastive representation learning," *Advances in neural information processing systems*, vol. 33, pp. 11142–11153, 2020.
- [17] Y. Bengio, P. Lamblin, D. Popovici, and H. Larochelle, "Greedy layer-wise training of deep networks," *Advances in neural information processing systems*, vol. 19, 2006.
- [18] H. Mostafa, V. Ramesh, and G. Cauwenberghs, "Deep supervised learning using local errors," *Frontiers in neuroscience*, vol. 12, p. 608, 2018.
- [19] Y. Dan and M.-m. Poo, "Spike timing-dependent plasticity of neural circuits," *Neuron*, vol. 44, no. 1, pp. 23–30, 2004.
- [20] Y. Bengio, D.-H. Lee, J. Bornschein, T. Mesnard, and Z. Lin, "Towards biologically plausible deep learning," *arXiv preprint arXiv:1502.04156*, 2015.
- [21] A. Krizhevsky, G. Hinton *et al.*, "Learning multiple layers of features from tiny images," 2009.
- [22] Y. Netzer, T. Wang, A. Coates, A. Bissacco, B. Wu, and A. Y. Ng, "Reading digits in natural images with unsupervised feature learning," 2011.
- [23] A. Coates, A. Ng, and H. Lee, "An analysis of single-layer networks in unsupervised feature learning," in *Proceedings of the fourteenth international conference on artificial intelligence and statistics. JMLR Workshop and Conference Proceedings*, 2011, pp. 215–223.
- [24] J. Deng, W. Dong, R. Socher, L.-J. Li, K. Li, and L. Fei-Fei, "Imagenet: A large-scale hierarchical image database," in *2009 IEEE conference on computer vision and pattern recognition*. Ieee, 2009, pp. 248–255.
- [25] S. Bartunov, A. Santoro, B. Richards, L. Marris, G. E. Hinton, and T. Lillicrap, "Assessing the scalability of biologically-motivated deep learning algorithms and architectures," *Advances in neural information processing systems*, vol. 31, 2018.
- [26] Y. Le Cun, "Learning process in an asymmetric threshold network," in *Disordered systems and biological organization*. Springer, 1986, pp. 233–240.
- [27] D.-H. Lee, S. Zhang, A. Fischer, and Y. Bengio, "Difference target propagation," in *Machine Learning and Knowledge Discovery in Databases: European Conference, ECML PKDD 2015, Porto, Portugal, September 7-11, 2015, Proceedings, Part I*. Springer, 2015, pp. 498–515.
- [28] T. P. Lillicrap, D. Cownden, D. B. Tweed, and C. J. Akerman, "Random feedback weights support learning in deep neural networks," *arXiv preprint arXiv:1411.0247*, 2014.
- [29] A. Nøkland, "Direct feedback alignment provides learning in deep neural networks," *Advances in neural information processing systems*, vol. 29, 2016.
- [30] M. Jaderberg, W. M. Czarnecki, S. Osindero, O. Vinyals, A. Graves, D. Silver, and K. Kavukcuoglu, "Decoupled neural interfaces using synthetic gradients," in *International conference on machine learning*. PMLR, 2017, pp. 1627–1635.
- [31] Z. Huo, B. Gu, and H. Huang, "Training neural networks using features replay," *Advances in Neural Information Processing Systems*, vol. 31, 2018.
- [32] Z. Huo, B. Gu, H. Huang *et al.*, "Decoupled parallel backpropagation with convergence guarantee," in *International Conference on Machine Learning*. PMLR, 2018, pp. 2098–2106.
- [33] G. DellaFerrera and G. Kreiman, "Error-driven input modulation: solving the credit assignment problem without a backward pass," in *International Conference on Machine Learning*. PMLR, 2022, pp. 4937–4955.
- [34] M. Ren, S. Kornblith, R. Liao, and G. Hinton, "Scaling forward gradient with local losses," *arXiv preprint arXiv:2210.03310*, 2022.
- [35] B. Illing, J. Ventura, G. Bellec, and W. Gerstner, "Local plasticity rules can learn deep representations using self-supervised contrastive predictions," *Advances in Neural Information Processing Systems*, vol. 34, pp. 30365–30379, 2021.
- [36] S. A. Siddiqui, D. Krueger, Y. LeCun, and S. Deny, "Blockwise self-supervised learning at scale," *arXiv preprint arXiv:2302.01647*, 2023.
- [37] Y. Xiong, M. Ren, and R. Urtasun, "Loco: Local contrastive representation learning," *Advances in neural information processing systems*, vol. 33, pp. 11142–11153, 2020.
- [38] S. Löwe, P. O'Connor, and B. Veeling, "Putting an end to end-to-end: Gradient-isolated learning of representations," *Advances in neural information processing systems*, vol. 32, 2019.
- [39] A. Journé, H. G. Rodriguez, Q. Guo, and T. Moraitis, "Hebbian deep learning without feedback," *arXiv preprint arXiv:2209.11883*, 2022.
- [40] E. Belilovsky, M. Eickenberg, and E. Oyallon, "Greedy layerwise learning can scale to imagenet," in *International conference on machine learning*. PMLR, 2019, pp. 583–593.
- [41] A. Nøkland and L. H. Eidnes, "Training neural networks with local error signals," in *International conference on machine learning*. PMLR, 2019, pp. 4839–4850.
- [42] Y. Wang, Z. Ni, S. Song, L. Yang, and G. Huang, "Revisiting locally supervised learning: an alternative to end-to-end training," *arXiv preprint arXiv:2101.10832*, 2021.
- [43] K. He, X. Zhang, S. Ren, and J. Sun, "Deep residual learning for image recognition," in *Proceedings of the IEEE conference on computer vision and pattern recognition*, 2016, pp. 770–778.
- [44] D. E. Rumelhart, G. E. Hinton, R. J. Williams *et al.*, "Learning internal representations by error propagation," 1985.
- [45] N. S. Keskar and R. Socher, "Improving generalization performance by switching from adam to sgd," *arXiv preprint arXiv:1712.07628*, 2017.

- [46] T. Dozat, “Incorporating nesterov momentum into adam,” 2016.
- [47] I. Loshchilov and F. Hutter, “Sgdr: Stochastic gradient descent with warm restarts,” *arXiv preprint arXiv:1608.03983*, 2016.
- [48] S. Kornblith, M. Norouzi, H. Lee, and G. Hinton, “Similarity of neural network representations revisited,” in *International conference on machine learning*. PMLR, 2019, pp. 3519–3529.
- [49] Z. Qu, H. Jin, Y. Zhou, Z. Yang, and W. Zhang, “Focus on local: Detecting lane marker from bottom up via key point,” in *Proceedings of the IEEE/CVF Conference on Computer Vision and Pattern Recognition*, 2021, pp. 14 122–14 130.